Developmental Biology 357 (2011) 392–403

Contents lists available at ScienceDirect

Developmental Biology

journal homepage: www.elsevier.com/developmentalbiology

Drosophila adducin regulates Dlg phosphorylation and targeting of Dlg to the synapse and epithelial membrane

Simon Wang [a,1], Jing Yang [b,1], Amy Tsai [b], Tomas Kuca [b], Justina Sanny [a,2], Jeehwa Lee [a], Kevin Dong [a], Nicholas Harden [a,*], Charles Krieger [b,*]

[a] Department of Molecular Biology and Biochemistry, Simon Fraser University, 8888 University Drive, Burnaby, British Columbia, Canada V5A 1S6
[b] Department of Biomedical Physiology and Kinesiology, Simon Fraser University, 8888 University Drive, Burnaby, British Columbia, Canada V5A 1S6

ARTICLE INFO

Article history:
Received for publication 15 November 2010
Revised 6 July 2011
Accepted 7 July 2011
Available online 23 July 2011

Keywords:
Adducin
Spectrin cytoskeleton
Neuromuscular junction
Dlg
Epithelial morphogenesis
Drosophila

ABSTRACT

Adducin is a cytoskeletal protein having regulatory roles that involve actin filaments, functions that are inhibited by phosphorylation of adducin by protein kinase C. Adducin is hyperphosphorylated in nervous system tissue in patients with the neurodegenerative disease amyotrophic lateral sclerosis, and mice lacking β-adducin have impaired synaptic plasticity and learning. We have found that *Drosophila* adducin, encoded by *hu-li tai shao* (*hts*), is localized to the post-synaptic larval neuromuscular junction (NMJ) in a complex with the scaffolding protein Discs large (Dlg), a regulator of synaptic plasticity during growth of the NMJ. *hts* mutant NMJs are underdeveloped, whereas over-expression of Hts promotes Dlg phosphorylation, delocalizes Dlg away from the NMJ, and causes NMJ overgrowth. Dlg is a component of septate junctions at the lateral membrane of epithelial cells, and we show that Hts regulates Dlg localization in the amnioserosa, an embryonic epithelium, and that embryos doubly mutant for *hts* and *dlg* exhibit defects in epithelial morphogenesis. The phosphorylation of Dlg by the kinases PAR-1 and CaMKII has been shown to disrupt Dlg targeting to the NMJ and we present evidence that Hts regulates Dlg targeting to the NMJ in muscle and the lateral membrane of epithelial cells by controlling the protein levels of PAR-1 and CaMKII, and consequently the extent of Dlg phosphorylation.

Introduction

To perform specific functions, eukaryotic cells have specialized membrane domains associated with regionally-restricted proteins that interact with a network of submembranous proteins that form the cytoskeleton. The actin cytoskeleton is composed of actin and spectrin filaments as well as actin and spectrin-interacting proteins that regulate the polymerization and depolymerization of actin and stabilize the association of the cytoskeleton with the plasma membrane. This basic cytoskeletal organization permits modification of the membrane at sites of cell–cell contact such as at the synapse or in epithelia (Ruiz-Canada and Budnik, 2006; Thomas, 2001).

Cell–cell contact is affected in neurodegenerative disorders that are characterized by the loss of specific neuronal populations. For example, in the disorder amyotrophic lateral sclerosis (ALS), also known as motor neuron disease, loss of synaptic contact between motor neurons and muscle is associated with motor neuron degeneration (Boillee et al., 2006; Parkhouse et al., 2008). We previously found that adducin, a spectrin and actin binding protein, is hyperphosphorylated in ALS patients and in a mouse model of ALS (Hu et al., 2003; Shan et al., 2005). Mammalian adducins comprise a family encoded by three closely related genes (α, β and γ), with the α and γ proteins being ubiquitously expressed and the β isoform abundant in the central nervous system (CNS) and erythrocytes (Bennett et al., 1988; Matsuoka et al., 2000). The adducins are composed of a globular N-terminal domain, a neck domain and, at the C-terminal, a myristoylated alanine-rich C-kinase substrate (MARCKS)-homology domain containing a serine residue that is a target for phosphorylation by protein kinase C (PKC). Adducin regulates actin filaments in several ways, including cross-linking with spectrin and capping of the barbed ends. These actin regulatory roles are inhibited by adducin phosphorylation in the MARCKS-homology domain, which causes adducin to translocate from the membrane to the cytosol (Matsuoka et al., 2000). In the mammalian nervous system, adducin immunoreactivity is localized to regions with high densities of synapses, such as the CA1 and CA3 regions of the hippocampus and at the terminals of parallel fibers in the cerebellum, and has also been observed in astroglia (Matsuoka et al., 1998; Seidel et al., 1995). We have found that phospho-adducin is expressed in neurons and glia of the mammalian CNS, as well as motor neurons (Shan et al., 2005).

To explore further the roles of adducin in the nervous system and cell adhesion we turned to *Drosophila*, with its well-characterized

* Corresponding authors.
E-mail addresses: nharden@sfu.ca (N. Harden), ckrieger@sfu.ca (C. Krieger).
[1] These authors contributed equally to this work.
[2] Present address: Developmental Biology Program, Sloan-Kettering Institute, New York, New York, 10021, USA.

0012-1606/$ – see front matter © 2011 Elsevier Inc. All rights reserved.
doi:10.1016/j.ydbio.2011.07.010

neuromuscular junction (NMJ) and advanced genetics. *Drosophila* orthologs of adducin are encoded by the *hu-li tai shao* ('too little nursing'; *hts*) locus, which has mainly been characterized with regard to its roles in oogenesis, although *hts* is expressed throughout development including in the embryonic CNS (Ding et al., 1993; Lin et al., 1994; Petrella et al., 2007; Whittaker et al., 1999; Yue and Spradling, 1992; Zaccai and Lipshitz, 1996a,b). Alternative splicing of *hts* products results in four distinct proteins with common N-terminal and neck domains but differing C-terminal regions. Two Hts proteins, Add1 and Add2, exhibit homology to mammalian adducin, where both have a MARCKS-domain in their C-terminal region (Petrella et al., 2007; Whittaker et al., 1999). Add2 differs from Add1 by the presence of an extra 23 amino acids in the C-terminal region. A third Hts protein, Ovhts, is a polyprotein with a novel C-terminal domain (RC), which undergoes cleavage during oogenesis, while a fourth protein, ShAdd, has a truncated C-terminal domain (Petrella et al., 2007).

In this study we demonstrate that Hts regulates the phosphorylation and localization of Dlg, a member of the membrane-associated guanylate kinase (MAGUK) family of scaffolding proteins that has important roles in the development and function of the NMJ (Budnik et al., 1996; Chen and Featherstone, 2005; Gorczyca et al., 2007; Guan et al., 1996; Koh et al., 1999; Lahey et al., 1994; Mendoza-Topaz et al., 2008; Tejedor et al., 1997; Thomas et al., 1997a,b; Zito et al., 1997). Dlg was originally isolated as a tumor suppressor gene regulating epithelial development in imaginal discs, and is an important determinant of apicobasal polarity as part of the Scribble complex, where it is incorporated into septate junctions during epithelial development (Woods and Bryant, 1989, 1991)(reviewed in (Humbert et al., 2008)). Hts co-localizes with Dlg at the post-synaptic membrane of the larval NMJ, and at the lateral membrane in epithelia, and exists in a complex with Dlg. Consistent with a role in regulating Dlg, Hts participates in synaptic growth, and the NMJ is underdeveloped in *hts* mutant larvae and overdeveloped following muscle-specific overexpression of Hts. Furthermore, *hts* interacts genetically with *dlg* during embryogenesis. We provide evidence that Hts affects Dlg phosphorylation by regulating the levels of two kinases, PAR-1 and CaMKII, which have been shown to phosphorylate Dlg and modify its localization at the NMJ (Koh et al., 1999; Zhang et al., 2007). Our finding that Hts regulates Dlg phosphorylation and localization at both the NMJ and at the epithelial membrane indicates conservation of Dlg regulation between tissues.

Materials and methods

Fly stocks

Unless otherwise indicated, stocks and crosses were raised at 25 °C using standard procedures. w^{1118} was used as the wild-type control for all experiments. *GS10063, GS13376* and *GS13858* were obtained from T. Aigaki and the *Drosophila* Gene Search Project, *mef2-Gal4* from S. Bahri. All other stocks were obtained from the Bloomington *Drosophila* Stock Center.

Immunohistochemistry and cuticle preparations

Body walls from late third instar larvae and embryos were fixed and immunostained for fluorescent imaging as described (Bellen and Budnik, 2000; Harden et al., 1996). Mutant body walls and embryos were distinguished by the lack of GFP balancer chromosomes. Fluorescent images were acquired with either a Zeiss LSM 410 laser-scanning confocal microscope or a Quorum spinning disk confocal microscope. For quantitative analysis of NMJ phenotypes, the glucose oxidase-DAB-nickel staining method (Hsu et al., 1988) was used and NMJs examined with a Leica TCS NT system. The following primary antibodies against Hts/adducin were used: monoclonal 1B1 anti-Hts (1:5)(Zaccai and Lipshitz, 1996a), htsM rabbit anti-Hts (1:200) (Petrella et al., 2007), and monoclonal anti-HtsRC (1:50)(Robinson et al., 1994). Other primary antibodies used were: rabbit anti-Hrp (1:500)(Jackson ImmunoResearch), monoclonal 4F3 anti-Dlg (1:5) (Parnas et al., 2001), monoclonal 6D6 anti-CSP-2 (1:250)(Zinsmaier et al., 1994), rabbit anti-p-Dlg (1:200)(Zhang et al., 2007), rabbit anti-CaMKII (1:1000)(Koh et al., 1999), rabbit anti-PAR-1 (1:200) (Tomancak et al., 2000) and rabbit anti-GFP (1:200)(Sigma). All secondary antibodies were from Vector Laboratories (1:200). Cuticle preparations were done as previously described (Harden et al., 1996). All images were processed in Adobe Photoshop.

Immunoprecipitations and Western blotting

To determine if Hts exists in a complex with Dlg, we performed reciprocal co-immunoprecipitation experiments on protein lysates prepared from 50 to 100 wild-type third-instar larvae. Immunoprecipitation with either monoclonal 4F3 anti-Dlg antibody or 1B1 anti-Hts antibody was performed essentially as described (Harlow, 1999). Samples were run on SDS-PAGE gels, blotted, and incubated with either 4F3 anti-Dlg antibody (1:1000) or 1B1 anti-Hts antibody (1:200) overnight at 4 °C (Sambrook et al., 1989). Bands were detected with HRP-conjugated secondary antibodies (Vector) using the ECL system (GE Healthcare). Anti-Dlg immunoprecipitations to quantify p-Dlg levels were performed similarly (using anti-p-Dlg at 1:1500), as were Western blots used to quantify Hts and Dlg levels. For quantification of Hts and Dlg levels, mouse anti-α-actin (1:1000) (Calbiochem) was used as a loading control. Band intensities on immunoblots were determined by performing densitometry using Adobe Photoshop CS4 as described (http://www.lukemiller.org/journal/2007/08/quantifying-western-blots-without.html).

Quantification of NMJ phenotypes

The muscle 6/7 NMJ in segment A4 of third instar larval body wall preparations stained with anti-CSP-2 antibodies was used for quantitative analysis of NMJ phenotypes. For each NMJ, the total number of boutons, branches and branch lengths was determined. To normalize data, we determined the surface area of muscle 6/7 for each NMJ using ImageJ software and calculated the average number of boutons, branches and branch lengths (in μm) per unit area ($5\times10^3\,\mu m^2$ for bouton numbers and branch length, and $5\times10^4\,\mu m^2$ for branch numbers). Student's t-test was used for statistical analysis and data expressed as the mean ± S.E.M.

Quantification of Dlg and p-Dlg levels in immunohistochemistry

For all quantitative analysis, samples were dissected, immunostained and imaged in parallel. Quantification of Dlg synaptic levels was calculated as a ratio between the fluorescence intensity of Dlg and Hrp, which was used as a control. Signal at the synapse was selected using Photoshop and the intensity was determined by measuring the mean gray value. Measurements were performed on two synapses (innervating muscles 6/7 from abdominal segments 3, 4 and 5) per body wall, with 12–14 third instar larvae of each genotype being examined. For quantification of punctate p-Dlg staining in the muscle, images were inverted and the threshold function of ImageJ was used to create binary images in which puncta were represented by black pixels (intensity of 255) and the background was eliminated. The number of black pixels in a defined area was measured from two sets of muscles 6/7 (from abdominal segments 3, 4 and 5) per body wall, with 10–15 individuals of each genotype being examined. Student's t-test was used for all statistical analysis and data expressed as the mean ± S.E.M.

Results

Hts localizes to the post-synaptic region of the NMJ

We examined the distribution of Hts at the *Drosophila* NMJ by double-labeling body walls of wild-type third instar larvae with anti-Hts and anti-Horseradish peroxidase (Hrp) antibodies. The anti-Hts antibody (1B1) used predominantly in this study detects every Hts isoform except ShAdd (Petrella et al., 2007; Zaccai and Lipshitz, 1996a), whereas the anti-Hrp antibody labels all neuronal membranes (Jan and Jan, 1982). In confocal analysis of the muscle 6/7 NMJ, Hts was found to localize to type Ib (b, big) and type Is (s, small) boutons (Fig. 1A-B′). Examination of muscles 12 and 13, which are innervated by all three types of boutons (i.e. I, II and III) (Gorczyca et al., 1993), showed that Hts only localized to type I (data not shown). Hts immunoreactivity at type I boutons was mostly localized circumferentially to the neuronal membrane marker indicating a post-synaptic distribution, although it has recently been reported that there is also pre-synaptic Hts at the NMJ (Pielage et al., 2011). We obtained similar results using an anti-Hts antibody (htsM) that detects the MARCKS domain of the Add1 and Add2 isoforms (Petrella et al., 2007)(Fig. 1B′). No NMJ immunoreactivity was observed with an anti-Hts antibody (htsRC) that detects the RC domain of the OvHts isoform (Petrella et al., 2007; Robinson et al., 1994)(data not shown). We conclude that Add1 and Add2, the *Drosophila* proteins most similar to mammalian adducins, are the predominant isoforms of Hts at the post-synaptic region of type I boutons.

Hts co-localizes with Dlg at the NMJ and at the epithelial lateral membrane and is in a complex with Dlg

The post-synaptic accumulation of Hts at type I boutons is reminiscent of the distribution of the important scaffolding molecule Dlg, which is dependent on the spectrin cytoskeleton for its NMJ localization, and we performed double labelings with anti-Hts and anti-Dlg (Featherstone et al., 2001; Lahey et al., 1994; Pielage et al., 2006). In analysis of muscles 6 and 7, which are innervated only by type I boutons, Hts co-localized with Dlg around the periphery of the boutons (Fig. 1B″). However, while Dlg immunoreactivity was more pronounced in type Ib boutons than type Is boutons (Fig. 1B) (Lahey et al., 1994), Hts was found at similar levels in both types (Fig. 1B). We were curious to compare the distribution of Hts and Dlg in epithelial cells, given the involvement of Dlg in apicobasal polarity and septate junction integrity. We examined the epidermis of dorsal closure stage embryos, when the epidermal flanks are migrating to close a hole in the epidermis occupied by an epithelium called the amnioserosa (Harden, 2002). A feature of Dlg and other septate junction proteins is that they are found along all epidermal lateral membranes with the exception of the leading edge (LE) of the dorsal-most epidermal (DME) cells that directly flank the dorsal hole (Fig. 1C) (Arquier et al., 2001; Bahri et al., 2010; Fehon et al., 1994; Grevengoed et al., 2001; Jacinto et al., 2000; Kaltschmidt et al., 2002; Wada et al., 2007). Similar to Dlg, Hts was excluded from the LE during dorsal closure but did not extend as far dorsally as Dlg in the DME cells (Fig. 1 C-C″), and

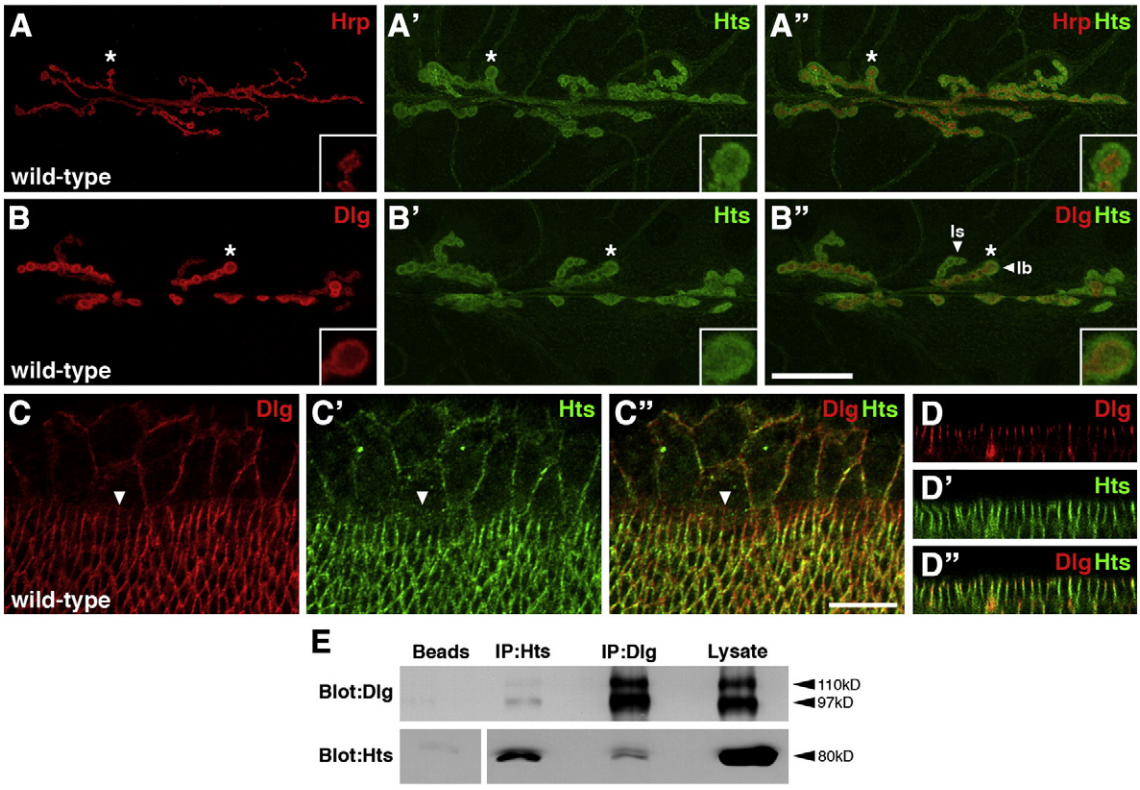

Fig. 1. Hts co-localizes with Dlg at the NMJ and in epithelia and exists in a complex with Dlg. Confocal microscope images in this and subsequent figures are shown as merged stacks. Boutons marked with an asterisk in panels A–B″ are shown at higher power in insets. (A–A″) Wild-type third instar larval NMJ innervating muscles 6/7 labeled with anti-Hrp (red), a neuronal membrane marker, and 1B1 anti-Hts (green). Hts localizes to the boutons, primarily around the periphery of the neuronal membrane indicating a post-synaptic distribution. (B–B″) Wild-type third instar larval NMJ innervating muscles 6/7 labeled with anti-Dlg (red), a post-synaptic marker, and htsM anti-Hts (green). Hts and Dlg co-localize around the periphery of type I boutons. However, Dlg immunoreactivity is higher in type Ib boutons than type Is boutons whereas Hts is found at similar levels in both type I boutons. (C–D″) Embryos undergoing dorsal closure were double-labeled with anti-Dlg (red) and htsM anti-Hts (green). (C) Dlg is excluded from the leading edge (LE) of the dorsal-most epidermal (DME) cells (arrowhead) as it migrates over the amnioserosa (top of figure). (C′, C″) Hts is similarly excluded from the LE, but is also absent from the dorsal ends of membranes between DME cells. (D-D″) Cross-sectional view of epidermal cells with apical surface at top of figure showing co-localization of Dlg and Hts in the lateral membrane, but with Hts extending more basally. (E) Immunoprecipitations using 1B1 anti-Hts antibody on third instar larval extracts pull down a Dlg doublet of 97 kD and 110 kD (upper panel, lane: IP:Hts). Reciprocal immunoprecipitations using an anti-Dlg antibody pull down an Hts doublet of 80 kD (lower panel, lane: IP:Dlg). No proteins were immunoprecipitated in controls using naïve beads. Scale bars, 50 μm (A–B″), 20 μm (C–C″).

immunolabelling of Hts overlapped with Dlg along lateral membranes, but extended more basally (Fig. 1 D-D˝).

hDlg, a human homolog of Dlg, binds protein 4.1 and may therefore be directly associating with the spectrin-actin junction, where protein 4.1 and adducin are both localized (Bennett and Gilligan, 1993; Lue et al., 1994; Lue et al., 1996). A similar situation could be occurring in *Drosophila*, indeed, Coracle, the *Drosophila* protein 4.1, is found at the post-synaptic NMJ and at the septate junction in epithelia, and Hts and Dlg could interact through a shared association with the spectrin-actin junction (Chen et al., 2005; Fehon et al., 1994). To determine if Hts exists in a complex with Dlg, we performed co-immunoprecipitation assays on wild-type third instar larval extracts. Hts immunoprecipitates blotted with anti-Dlg antibodies revealed two bands of about 97 kDa and 110 kDa (Fig. 1E, top panel), consistent with the size of Dlg isoforms previously detected in larval body walls (Lahey et al., 1994). In reciprocal co-immunoprecipitation assays, immunoprecipitated Dlg blotted with anti-Hts (1B1) antibodies revealed a doublet of approximately 80 kDa, which corresponds to the predicted size of the Add1 and Add2 isoforms of Hts (Petrella et al., 2007)(Fig. 1E, bottom panel). We found that the anti-Hts (1B1) antibody was poor at immunoprecipitating Hts, whereas the anti-Dlg antibody was effective at pulling down Dlg. Dlg pull downs indicated that a small proportion of the adducin-like isoforms of Hts was present in a complex with Dlg in the larva, consistent with our immunohistochemistry showing that Hts has a more extensive distribution at the epithelial membrane than Dlg.

Hts regulates NMJ development and controls Dlg localization at the NMJ and in epithelia

To evaluate a potential role for Hts during NMJ development, we examined Hrp- and Dlg-stained muscle 6/7 NMJs in third instar larvae mutant for two P-element insertion alleles of *hts*, hts^{01103} and hts^{k06121} (Fig. 2A)(Berkeley *Drosophila* Genome Project)(Spradling et al., 1999). With both alleles, NMJs were clearly underdeveloped in terms of branching (Compare Fig. 3A to Fig. 3B and data not shown). A previous study of *hts* function in testes produced the allelic series $hts^{01103} > hts^{1} > hts^{KG06777} > hts^{k06121}$ based on phenotype and immunoblot analysis, with hts^{01103} being the most severe allele (Wilson, 2005). Consistent with these findings, hts^{k06121} individuals showed some retention of Hts immunoreactivity at the NMJ, while hts^{01103} larvae lacked NMJ Hts immunostaining and were used for further analysis (Fig. 2C and data not shown). We confirmed by immunoblot analysis that hts^{01103} larval body walls had no detectable Hts protein (Fig. 2E). The hts^{01103} allele is pharate adult lethal but survives as a hemizygote over the deficiency *Df(2R)BSC26*, which removes *hts* (Wilson, 2005). We chose not to perform NMJ analysis on *hts* hemizygotes over *Df(2R)BSC26* as these larvae would be hemizygous for *coracle*, which encodes a component of the spectrin cytoskeleton participating in NMJ development (Chen et al., 2005). We are confident that the NMJ defects seen in hts^{01103} homozygotes are due to loss of Hts and not to a second site mutation as an independently generated allele, hts^{k06121}, shows the same NMJ phenotype (data not shown).

We determined by immunoblot analysis that hts^{01103} mutant larval body walls did not have a significant alteration in the overall levels of Dlg compared to wild-type (Fig. 3E). We then quantified Dlg localization at the NMJ in hts^{01103} mutants relative to wild-type by standardizing anti-Dlg staining intensity against Hrp staining intensity and found that there were lower levels of Dlg at the NMJ in hts^{01103} mutants, although Dlg remained tightly localized at the NMJ (Fig. 3B′, F). We explored further the participation of Hts in NMJ development and Dlg localization using over-expression. *hts* was over-expressed post-synaptically by crossing three Gene Search (GS) element insertion lines, *GS10063*, *GS13376* and *GS13858* (Fig. 2A) (Toba et al., 1999) bearing UAS sequences upstream of the endogenous *hts* gene, to the muscle-specific *mef2-Gal4* driver (Ranganayakulu et al., 1998) and third instar larval NMJs were assessed by co-staining with anti-Hrp and either anti-Hts and anti-Dlg. All three crosses exhibited over-expression of *hts* in muscle and in all cases NMJs were clearly overgrown (Fig. 2D, Fig. 3C and data not shown). We used *GS13858* for all further analysis of Hts over-expression. With *mef2-Gal4* driven over-expression of *hts* from *GS13858*, Dlg became delocalized from the NMJ in a diffuse pattern (Fig. 3C′) reminiscent of that seen with excessive phosphorylation of Dlg by CaMKII or PAR-1 (Koh et al., 1999; Zhang et al., 2007). By comparison with Hrp staining we confirmed that there was less Dlg localization at boutons in these NMJs than in wild-type (Fig. 3F). We used Western blot analysis of larval body walls to look at the levels of Dlg in these individuals and found no change in total Dlg levels (Fig. 3E). Given that Hts over-expression causes delocalization of Dlg from the NMJ it is perhaps surprising that we found reduced Dlg levels at the NMJ in hts^{01103} mutants. A likely explanation is the recent finding that the subsynaptic reticulum, where post-synaptic Dlg localizes at the NMJ (Lahey et al., 1994), is disrupted in *hts* mutants (Pielage et al., 2011).

Given the partial co-localization of Hts and Dlg in the embryo, we determined if Hts regulated Dlg localization in embryonic epithelia, as in muscle. We could not discern a change in Dlg distribution in hts^{01103} embryos compared to wild-type (data not shown), but over-expression of *hts* from *GS13858* using *prd-Gal4*, which produces stripes of expression extending from the epidermis into the amnioserosa, caused

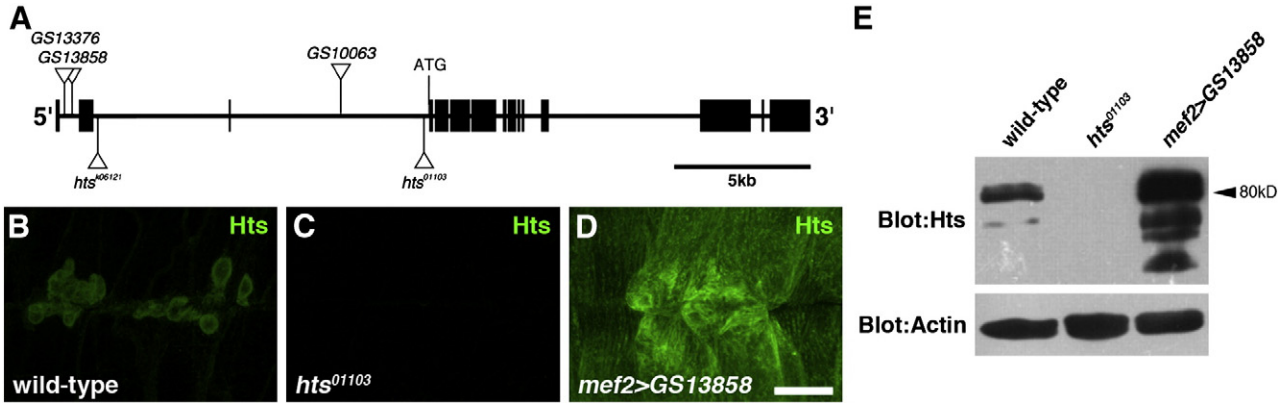

Fig. 2. P element insertions used to study Hts function. (A) The *hts* gene. Exons and introns are indicated as vertical and horizontal bars, respectively. The positions of transposon insertions are indicated with triangles. (B–D) Comparison of 1B1 anti-Hts immunoreactivity in NMJs of wild-type, hts^{01103} mutant and embryos in which wild-type Hts has been over-expressed in the muscle by crossing *mef2-Gal4* to *GS13858*. (E) Western blot analysis on extracts from larval body walls showing lack of Hts in hts^{01103} mutants and elevated Hts protein in *mef2>GS13858* larvae compared to wild-type. An actin antibody was used as a loading control. Scale bar, 20 μm.

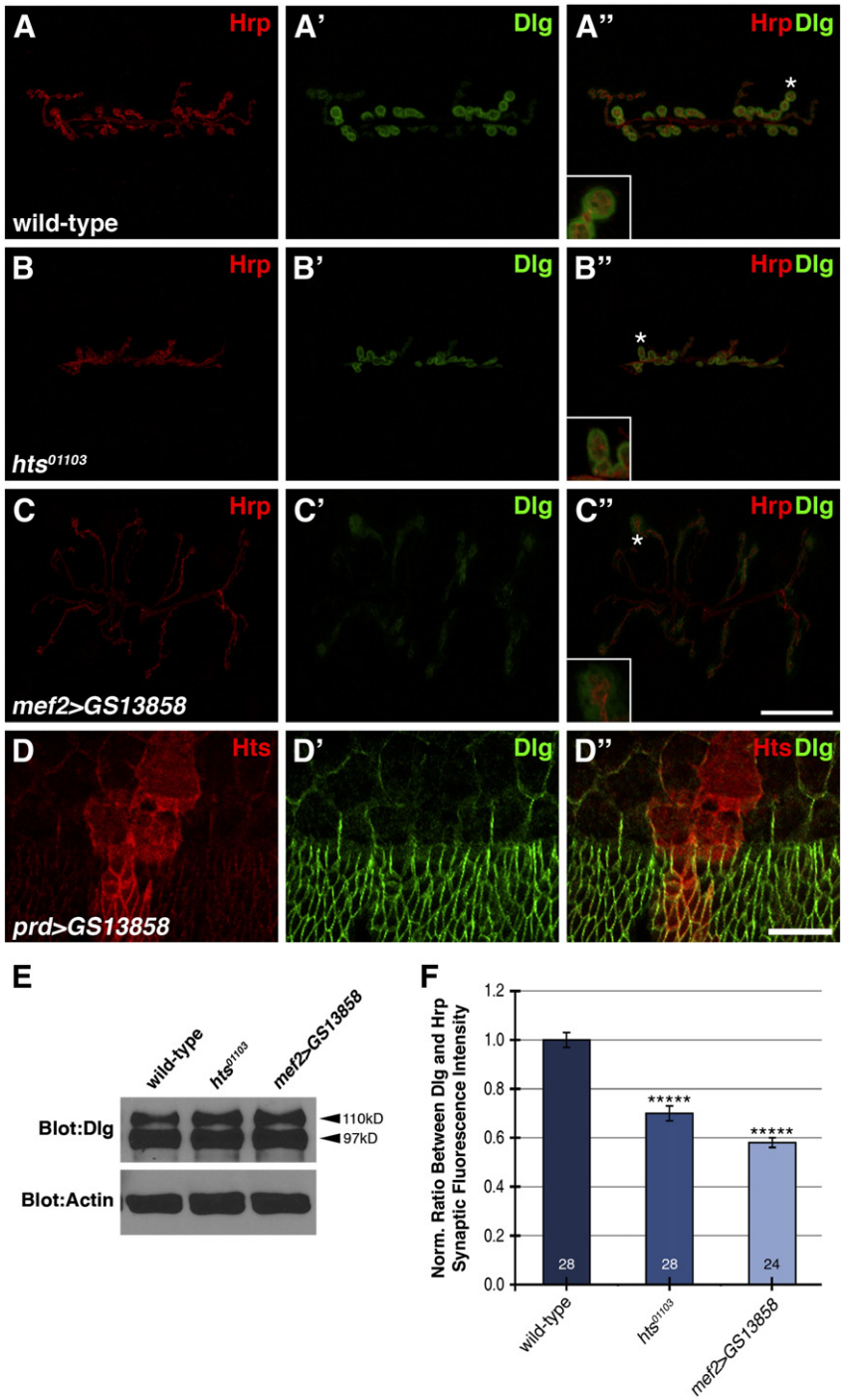

Fig. 3. Hts regulates Dlg targeting to the NMJ and lateral membrane in amnioserosa epithelial cells but does not regulate overall Dlg levels. (A–C˝) Third instar larval NMJs innervating muscles 6/7 double-labeled with anti-Hrp (red) and anti-Dlg (green). Boutons marked with an asterisk in panels A˝, B˝ and C˝ are shown at higher power in insets. (A-A˝) Dlg localizes to the post-synaptic membrane of wild-type NMJs. (B-B˝) hts^{01103} mutant NMJs are underdeveloped but Dlg remains localized to the NMJ. (C-C˝) Muscle-specific over-expression of wild-type Hts from *GS13858* causes NMJ overgrowth and disrupts Dlg post-synaptic targeting with Dlg exhibiting a diffuse distribution extending beyond the NMJ. (D-D˝) Over-expression of Hts in *prd* stripes in the embryo disrupts cortical localization of Dlg in the amnioserosa but not in the epidermis. (E) Western blot of lysates prepared from third instar larval body walls. Dlg protein levels in hts^{01103} mutant and *mef2>GS13858* larvae are similar to wild-type. This experiment was repeated 3 times and Dlg levels determined by densitometry and normalized to actin levels. No significant differences in Dlg levels were seen between the three genotypes (data not shown). (F) Comparison of Dlg staining levels to Hrp staining levels demonstrates that hts^{01103} mutant and *mef2>GS13858* larvae have lower levels of Dlg at boutons than in wild-type. Numbers on bars of graph indicate number of NMJ evaluated for each genotype. *****$p<0.0001$. Scale bars, 30 μm (A–C˝), 20 μm (D–D˝).

a reduction in cortical Dlg staining in amnioserosa cells but not in the epidermis (Fig. 3 D-D˝). We conclude that Hts is capable of delocalizing Dlg from the both the NMJ and the amnioserosa cell membrane during development.

In order to perform a quantitative assessment of hts^{01103} and *hts* over-expression growth NMJ defects, we immunolabelled wild-type, mutant and *hts*-over-expressing third instar body wall preparations with an antibody against CSP-2, a major component of synaptic vesicles (Zinsmaier et al., 1994)(Fig. 4 A–C), and determined bouton and branch number, as well as branch lengths, in muscle 6/7 NMJs of wild-type and mutant larvae. NMJs of hts^{01103} mutants had significantly fewer and shorter branches, but no significant difference in

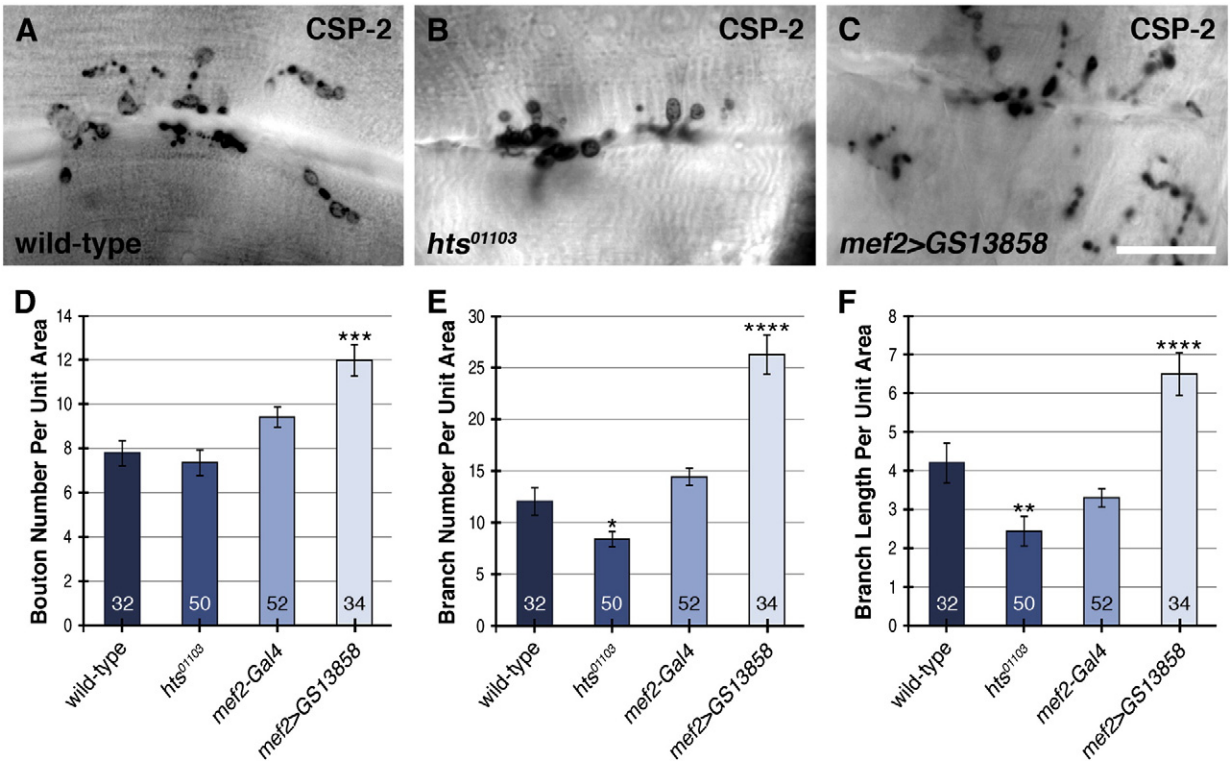

Fig. 4. Hts regulates bouton numbers, branch number and branch length at the NMJ. (A) Third instar larval NMJs innervating muscles 6/7 labeled with anti-CSP-2 showing typical wild-type (A), hts^{01103} mutant (B) and Hts over-expressing (C) NMJs used in quantitative analysis. (D-F) Results of quantitative analysis. hts^{01103} mutant larvae have significantly fewer and shorter branches, while Hts over-expressing individuals have significantly more and longer branches, as well as a greater number of boutons. Numbers on bars of graph indicate number of NMJs evaluated for each genotype. As the two NMJS in segment A4 of each body wall were examined, the number of individuals examined for each genotype is half. *$p<0.05$, **$p<0.01$, ***$p<0.005$, ****$p<0.001$. Scale bar, 30 μm.

bouton number, whereas muscle-specific over-expression of *hts* using *GS13858* resulted in significant increases in bouton number, branch number, and branch length (Fig. 4 D–F).

Hts interacts with Dlg during embryonic epithelial development

Our results suggest that Hts is regulating Dlg in epithelial cells in addition to the NMJ. Gross defects in epithelial morphogenesis can be detected using embryonic cuticle preparations, and we used this approach to study the development of *hts* mutant embryos. Cuticle preparations of *hts* mutant stocks had a higher frequency of morphological defects than seen in wild-type control embryos, indicating that some *hts* mutant embryos died with defects in embryogenesis (Fig. 5A). A variety of cuticle defects were seen in *hts* mutant stocks, but most prevalent were defects in the head, indicating problems with head involution and embryos that had only secreted a small amount of cuticle, indicating a disruption of epithelial integrity. If Hts is modulating Dlg localization during epithelial development, we reasoned that *hts* and *dlg* should interact genetically in the embryo and we looked for such an interaction by making double mutants. We chose two alleles of *dlg* that are post-embryonic lethal (Peter et al., 2002), and assessed the effects on embryogenesis of making embryos doubly mutant for hts^{01103} and *dlg*. In these crosses, the frequency of cuticle defects was substantially higher than crosses involving either the *hts* allele alone or a *dlg* allele alone, indicating a genetic interaction between *hts* and *dlg* (Fig. 5A). In the double mutant crosses the most common defects were again head holes and failure to secret cuticle (Fig. 5C, D). The frequency of defects was consistent with many individuals homozygous mutant for one gene and heterozygous for the other dying during embryogenesis. Interestingly, when the hts^{01103} allele was placed over the deficiency *Df(2R)BSC26*, which removes *hts*, the frequency of cuticle defects increased compared to the hts^{01103} stock, even though hts^{01103} appears to be a protein null allele. One possibility is that heterozygosity for *coracle* in the deficiency cross was having an effect on the *hts* phenotype.

The Hts/Dlg interactions we identified in epithelial development prompted us to investigate whether Dlg had any effect on Hts distribution in epithelia. We looked at Hts immunoreactivity in dlg^{G0342} and dlg^{G0456} mutant embryos, and while there were indications of subtle effects on Hts distribution the results were not consistent (data not shown). However, when analyzing embryos mutant for a third post-embryonic lethal *dlg* allele, dlg^{G0276} (Peter et al., 2002), we did find a consistent effect on Hts distribution. Compared with their balancer chromosome-bearing siblings, dlg^{G0276} mutant embryos showed disruption of cortical Hts localization in the amnioserosa of embryos early in dorsal closure, showing considerable punctate, cytoplasmic Hts staining (Fig. 5E, F). The Hts distribution in the epidermis, however, remained largely cortical in dlg^{G0276} mutant embryos, although there were some cytoplasmic puncta.

Hts promotes Dlg phosphorylation in muscle and epithelial cells

The delocalization of Dlg caused by Hts over-expression is similar to that seen following phosphorylation of Dlg at the NMJ by the CaMKII and PAR-1 kinases, and we determined whether Hts was promoting Dlg phosphorylation using an antibody that recognizes Dlg phosphorylated on serine 797 (p-Dlg), the site phosphorylated by PAR-1 (Koh et al., 1999; Zhang et al., 2007). Wild-type body wall preparations showed a punctate pattern of p-Dlg staining, with the frequency of puncta varying considerably between individuals, suggesting dynamic regulation of Dlg phosphorylation (Fig. 6A, D). Compared to wild-type, hts^{01103} mutant body walls showed a decrease in the number of p-Dlg puncta, whereas there was an increase in the intensity of p-Dlg puncta in body walls in which *mef2-Gal4* had been used to drive over-expression of *hts* from *GS13858*

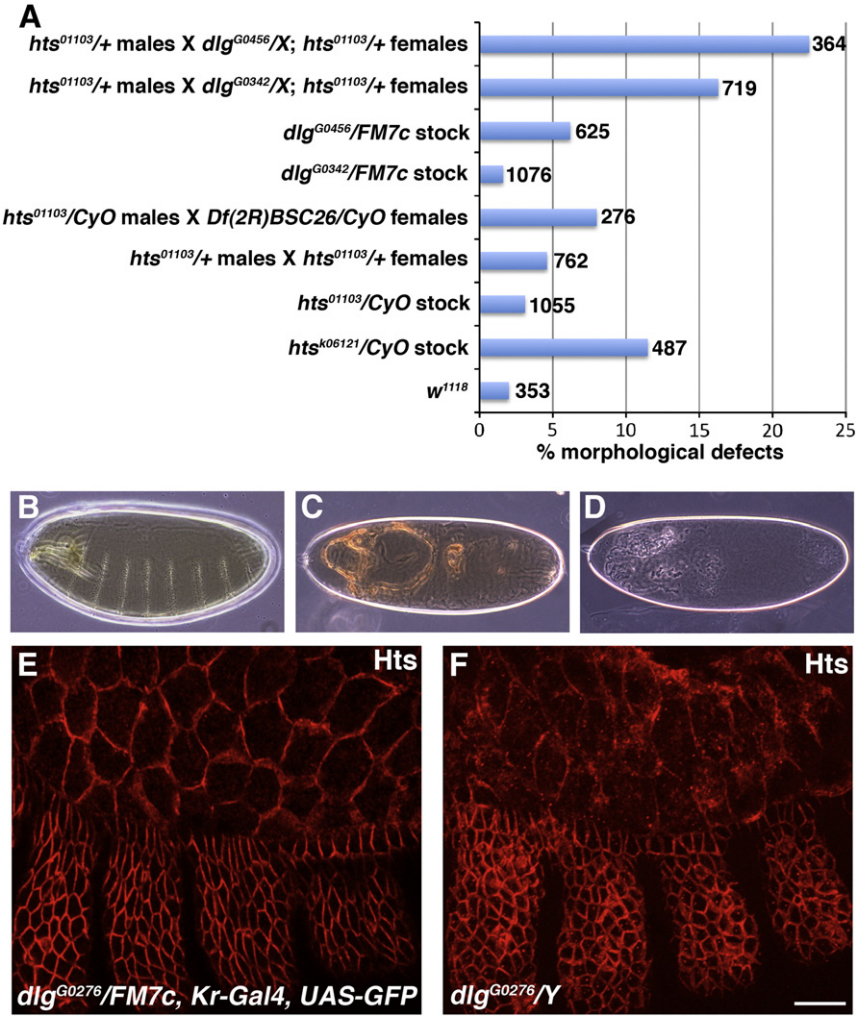

Fig. 5. Interactions between Hts and Dlg during epithelial development. (A) Graph showing frequencies of morphological defects in cuticle preparations from crosses bearing *hts* and *dlg* alleles. The cross or stock used for each preparation is indicated to the left of each bar on the graph. Numbers to the right of each bar indicate total number of cuticles examined. (B) Lateral view of wild-type embryonic cuticle from w^{1118} stock. (C, D) Most prevalent defects in double mutant crosses are a head open phenotype (C) and the secretion of only small pieces of cuticle (D). These embryos are from the dlg^{G0342} hts^{01103} double mutant cross. (E) Anti-Hts immunostaining of dlg^{G0276}/*FM7c, Kr-Gal4, UAS-GFP* embryo early in dorsal closure showing robust cortical accumulation of Hts in the amnioserosa and epidermis. Embryo was genotyped by detection of balancer with anti-GFP immunostaining (data not shown). (F) Similarly aged dlg^{G0276} mutant embryo, imaged under identical conditions as its sibling in (E), showing disruption of Hts cortical localization in the amnioserosa. There is strong cortical localization in the epidermis, although some cytoplasmic puncta are visible. Scale bar, 20 μm (E, F).

(Fig. 6 A–C). The overall intensity of p-Dlg staining in body wall preparations of the three genotypes was determined by counting the number of black pixels in a defined area of inverted images, and hts^{01103} mutants were found to have significantly lower levels and *mef2>GS13858* individual significantly higher levels (Fig. 6D). We further assessed p-Dlg levels by immunoprecipitating Dlg from bodywall preparations and Western blotting with anti-p-Dlg (Fig. 6E). Densitometry using anti-Dlg as a loading control indicated that *mef2>GS13858* body walls had about three times the levels of p-Dlg as wild-type, whereas hts^{01103} samples showed a 30% decrease. To determine if Hts was capable of promoting Dlg phosphorylation in epithelial cells as in muscle, we over-expressed Hts from *GS13858* using *prd-Gal4* and found elevated levels of p-Dlg in *prd* stripes (Fig. 6 F-F´). We conclude that Hts promotes phosphorylation of Dlg in both muscle and epithelial cells.

Hts promotes accumulation of PAR-1 and CaMKII in muscle and epithelial cells

The effects of Hts on Dlg localization and phosphorylation suggested Hts-mediated regulation of kinase(s) phosphorylating Dlg and we therefore looked at the distribution of PAR-1 and CaMKII in individuals with losses or gains of Hts function. *hts* mutant body wall preparations had a different pattern of PAR-1 and CaMKII immunoreactivity than in wild-type, suggesting an effect on kinase distribution and/or levels (Fig.7A, B, D, E). With *mef2-Gal4*-driven over-expression of *hts* from *GS13858* there was a substantial increase in both PAR-1 and CaMKII immunoreactivity throughout the muscle (Fig. 7C, F). To determine if this regulation of kinase levels was conserved in epithelial cells, we over-expressed Hts from *GS13858* using *prd-Gal4* and found elevated levels of PAR-1 and CaMKII in *prd* stripes. In the case of PAR-1 an increase in PAR-1 immunoreactivity was seen in both the epidermis and amnioserosa (Fig. 7 G-G´´), whereas CaMKII elevation was most notable in the amnioserosa and only slight or not obvious in the epidermis (Fig 7 H-H´´ and data not shown). We conclude that Hts regulates PAR-1 and CaMKII levels in both muscle and epithelial cells and as a consequence affects the phosphorylation and localization of Dlg.

Discussion

Dlg is a *Drosophila* member of a family of MAGUK scaffolding proteins that has four mammalian members, SAP97/hDlg, PSD-93/Chapsyn-110, PSD-95/SAP90 and SAP102/NE-Dlg, and which has important

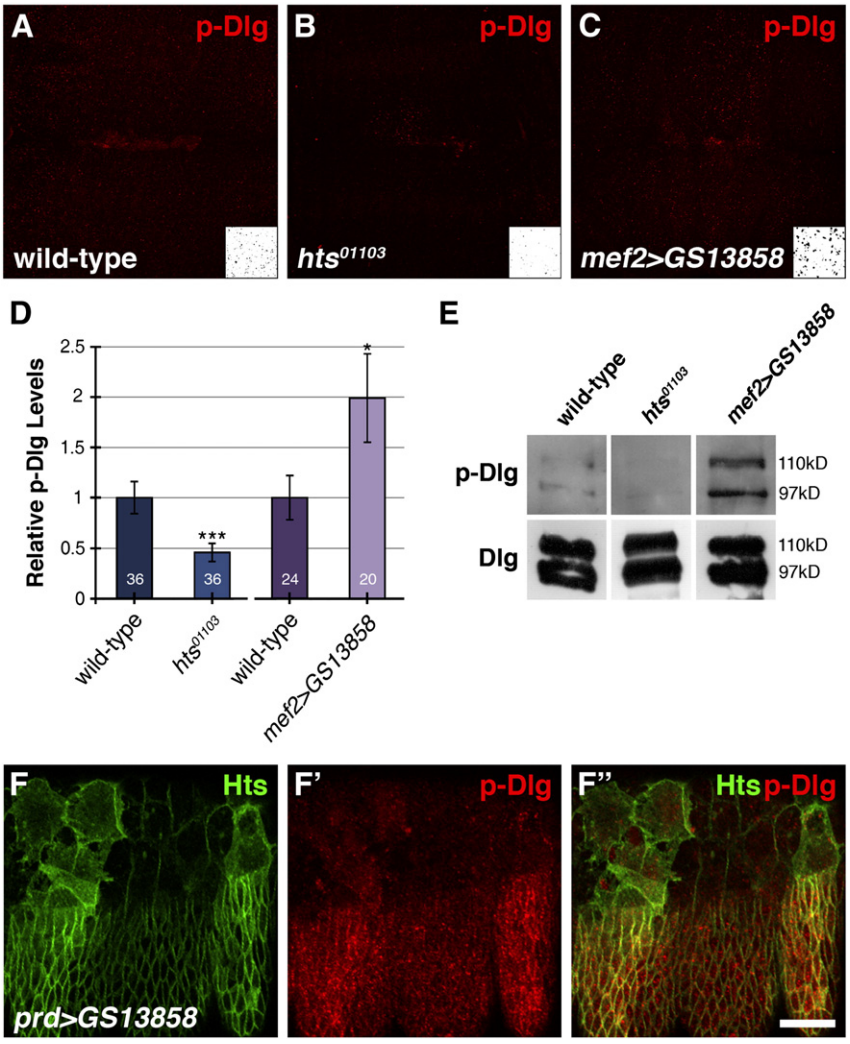

Fig. 6. Hts regulates Dlg phosphorylation. (A-C) Third instar larval NMJs innervating muscles 6/7 immunostained with anti-p-Dlg. Compared to wild-type (A) *hts*^{01103} mutants have fewer p-Dlg puncta (B), whereas *mef2>GS13858* larvae have more intense p-Dlg puncta (C). These differences are obvious in the inverted images shown in the insets. (D) Quantification of levels of p-Dlg puncta in immunohistochemistry of body wall preparations, calculated using inverted images. *hts*^{01103} mutants and *mef2>GS13858* body walls were compared to wild-type body walls that had been prepared and imaged in parallel. Wild-type levels have been set to a value 1 for each comparison. (E) Dlg was immunoprecipitated from extracts of third instar larval body wall preparations and Western blotted. Top panels show anti-p-Dlg staining, bottom panels show same blot after stripping and immunolabeling with anti-Dlg. (F-F″) Similar to what is seen in muscle, over-expression of wild-type Hts using *GS13858* in *prd* stripes in the epidermis and amnioserosa (tissue at top of figure) causes elevation of p-Dlg levels.

developmental and regulatory roles in the nervous system and in epithelia (Humbert et al., 2008; Thomas et al., 2010). Phosphorylation is emerging as a mechanism for the regulation of the localization and function of the Dlg family. The post-synaptic targeting of Dlg to the *Drosophila* NMJ is inhibited by phosphorylation of the first PDZ domain by CaMKII and of the GUK domain by PAR-1 (Koh et al., 1999; Zhang et al., 2007). In mammalian neurons, CaMKII phosphorylation of PDZ1 of PSD-95 terminates long term potentiation-induced spine growth by inducing translocation of PSD-95 out of the active spine (Steiner et al., 2008). Furthermore, phosphorylation of PDZ1 of either PSD-95 or SAP97/hDlg by CaMKII regulates their interaction with NMDA subunits, and additional cell culture studies in epithelial cells demonstrate effects of SAP97/hDlg phosphorylation by various kinases (Gardoni et al., 2003, 2006; Mantovani and Banks, 2003; Massimi et al., 2006; Narayan et al., 2009; Sabio et al., 2005).

An important function of Dlg at the NMJ is involvement in synaptic plasticity during muscle growth, at least in part by controlling the localization at the pre-synaptic and post-synaptic membranes of Fas2, a homophilic cell adhesion molecule of the immunoglobulin superfamily that binds Dlg (Koh et al., 1999; Thomas et al., 1997a; Zito et al., 1997). The breaking and restoration of Dlg/Fas2-mediated adhesion between the pre- and post-synaptic membranes is likely critical to synaptic growth during development (reviewed in (Ataman et al., 2006)). We have shown that Hts exists in a complex with Dlg, probably at both the post-synaptic membrane of the NMJ and at the lateral membrane in epithelia, where the two proteins are likely brought into close proximity by a shared association with the spectrin-actin junction. Hts is therefore positioned to locally regulate Dlg and participate in synaptic plasticity at sites of association with the membrane cytoskeleton, and it positively contributes to phosphorylation of Dlg on its GUK domain (see model in Fig. 8). This site of phosphorylation is a target for PAR-1, and consistent with this we find that Hts can regulate the levels of PAR-1. Phosphorylation of Dlg impedes its targeting to the post-synaptic membrane and we propose that Hts regulates this targeting at the synapse by controlling the levels of PAR-1 at the post-synaptic membrane (Zhang et al., 2007). This could occur through Hts acting as a scaffold participating in localized stabilization or translation of PAR-1 at the post-synaptic membrane and, consistent with the latter mechanism, localized post-synaptic translation of NMJ proteins has been reported in *Drosophila* (Sigrist et al., 2000). We have shown that over-expression of Hts permits

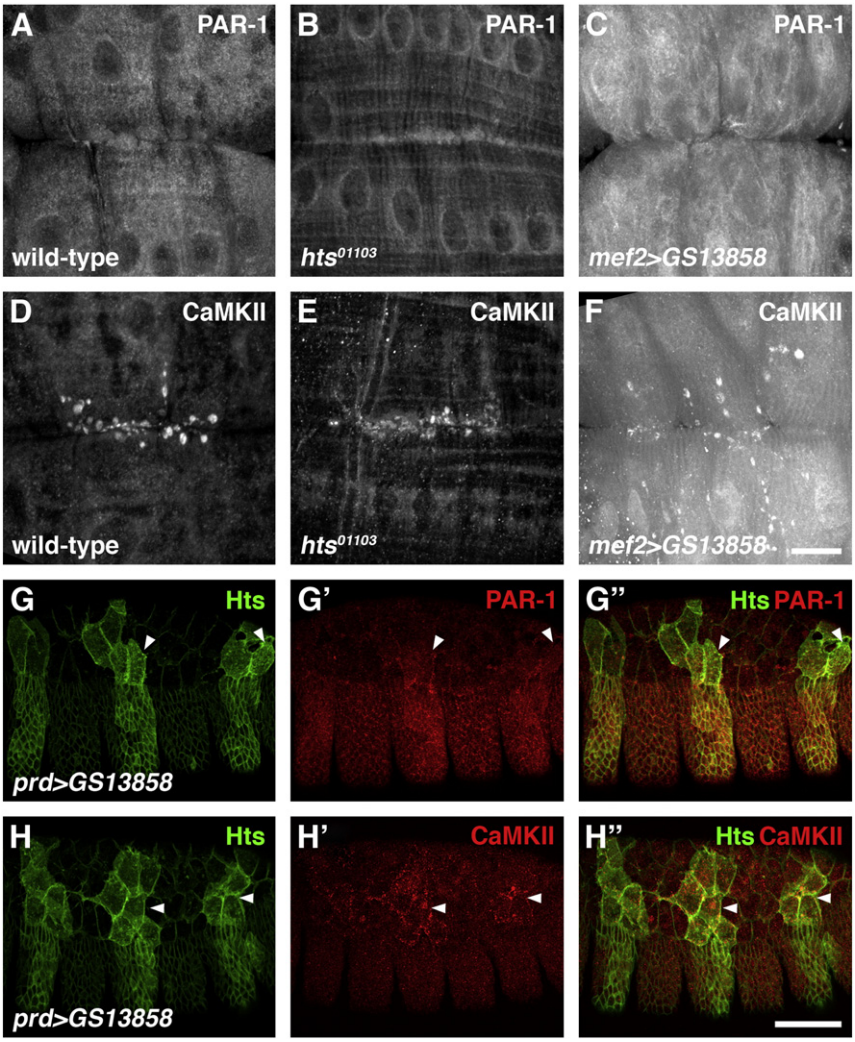

Fig. 7. Hts regulates PAR-1 and CaMKII levels in muscle and epithelial cells. (A-F) Third instar larval NMJs innervating muscles 6/7 immunostained with anti-PAR-1 (A-C) or anti-CaMKII (D-F). (A) Wild-type body wall showing fairly uniform distribution of PAR-1 immunostaining. hts^{01103} mutants (B) have a PAR-1 immunostaining pattern distinct from wild-type, whereas *mef2>GS13858* larvae have increased levels of PAR-1 immunoreactivity (C). (D) Wild-type body wall showing enrichment of CaMKII at NMJ and uniform distribution of CaMKII immunostaining elsewhere in the muscle. Compared to wild-type hts^{01103} mutants have reduced CaMKII immunostaining at the NMJ (E), whereas *mef2>GS13858* larvae have increased levels of CaMKII immunoreactivity (F). (G-H˝) Over-expression of wild-type Hts using *GS13858* in *prd* stripes in the epidermis and amnioserosa (tissue at top of figure) causes elevation of PAR-1 immunostaining in both these tissues (G΄, G˝) and increases CaMKII immunoreactivity in the amnioserosa (H΄, H˝). Scale bars, 20 μm (A-F), 40 μm (G–H˝). Arrowheads mark examples of amnioserosa cells showing elevated levels of PAR-1 (G–G˝) or CaMKII (H–H˝).

synaptic overgrowth, which may in part be due to effects on Dlg targeting to the post-synaptic membrane but we have unpublished results indicating additional routes of action. Furthermore, if Hts were acting mainly by elevating PAR-1 levels we would expect to see synaptic undergrowth rather than overgrowth with Hts over-expression, as the post-synaptic over-expression of PAR-1 leads to decreased bouton number and an oversimplified synapse (Zhang et al., 2007). CaMKII also regulates synaptic growth and Dlg targeting at the NMJ through phosphorylation (Koh et al., 1999). There is currently no antibody available to examine phosphorylation of Dlg by CaMKII in vivo, but we determined that Hts controls the levels of this kinase similarly to PAR-1, suggesting that Hts may also be regulating Dlg targeting via CaMKII-dependent phosphorylation (Fig. 8).

While this paper was under revision, two studies were published on Hts function in neurons, one describing a role in photoreceptor axon guidance and the other characterizing pre-synaptic Hts function at the NMJ (Ohler et al., 2011; Pielage et al., 2011). The latter study reported a phenotype of synaptic retraction at the *hts* mutant NMJ, revealed by the absence of the pre-synaptic marker Bruchpilot from extensive stretches of the NMJ, which is consistent with our observation of small synapses in *hts* mutants stained for the synaptic vesicle marker CSP-2 (Pielage et al., 2011). However, in addition to retraction, this group observed overgrowth of the *hts* mutant NMJ, visible with anti-HRP staining. Although we didn't do any quantification using anti-HRP, qualitative examination of our *hts* mutant muscle 6/7 NMJs did not indicate an overgrowth phenotype. A possible explanation for this discrepancy is our choice of the muscle 6/7 NMJ for analysis in contrast to Pielage et al. who focused on muscle 4. Unlike most other larval muscles, muscles 6 and 7 are not innervated by type II boutons (Johansen et al., 1989; Monastirioti et al., 1995). A component of the synaptic overgrowth reported by Pielage et al. is the extension of thin, actin-rich extensions somewhat similar in appearance to type II and type III processes and, accordingly, growth of these processes is impaired with pre-synaptic over-expression of Hts (Pielage et al., 2011). These authors propose that pre-synaptic Hts restricts synaptic growth through its function as an actin-capping protein. At the muscle 6/7 NMJ this role may not be so prevalent and the post-synaptic growth-promoting function of Hts prevails. By examining NMJs other than muscle 6/7 in our *hts* mutant larvae we were able to confirm the overgrowth phenotype observed by Pielage et al. (N. H., unpublished observations).

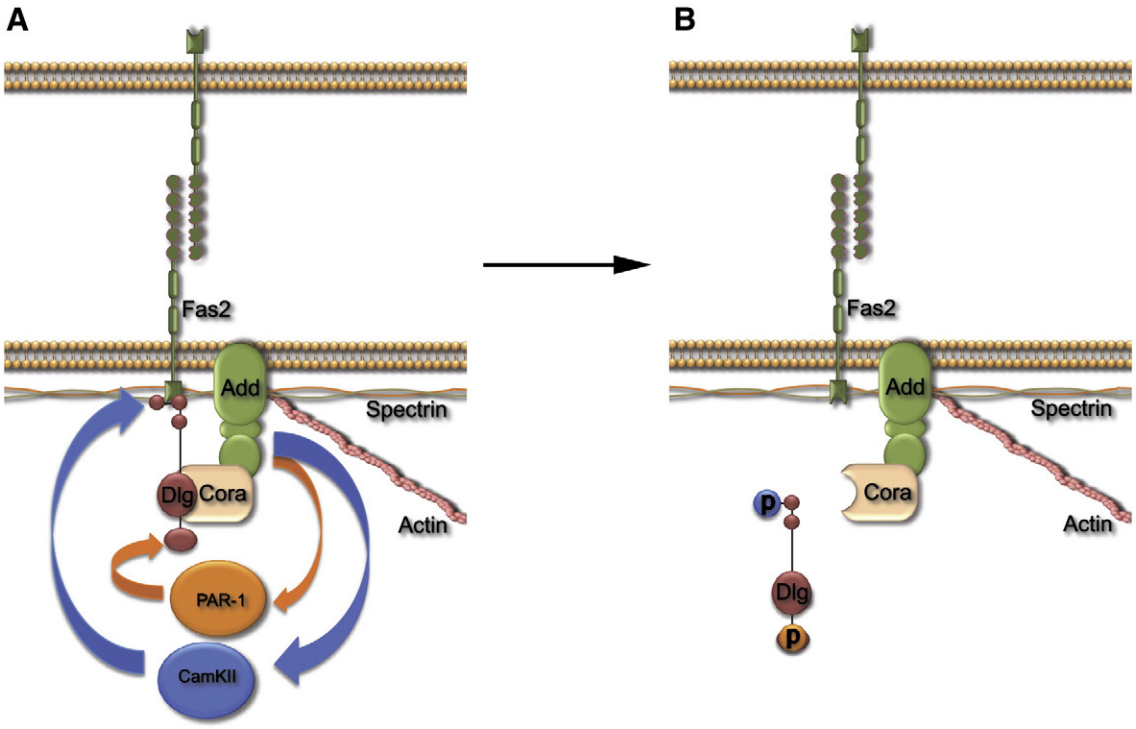

Fig. 8. Model for Hts regulation of Dlg at the NMJ. Model shows a lateral view of an NMJ. The presynaptic membrane is shown at top of figure. (A) Dlg is localized to spectrin-actin junctions, possibly through binding to Coracle. Homophilic adhesion between Fas2 molecules links the pre-synaptic and post-synaptic membranes, with the intracellular domain of Fas2 anchored to Dlg. Hts forms a complex with Dlg through association with the spectrin–actin junction, where it promotes the accumulation of PAR-1 and CaMKII, which phosphorylate Dlg on the GUK and PDZ1 domains, respectively. (B) Phosphorylated Dlg becomes delocalized from the NMJ, disrupting Fas2-mediated adhesion between the pre-synaptic and post-synaptic membranes, and enabling synaptic plasticity.

Synaptic plasticity at the *Drosophila* NMJ has parallels with the structural changes seen at synapses in cellular models of learning such as long-term facilitation (LTF) in *Aplysia* and long-term potentiation in the mammalian hippocampus (Schuster et al., 1996), and several studies indicate that our results with *hts* at the NMJ may be relevant to these other systems. Phosphorylation of the conserved serine residue in the MARCKS domain of adducin is increased during LTF in Aplysia, and mice lacking β-adducin exhibit impaired synaptic plasticity and learning (Bednarek and Caroni, 2011; Gruenbaum et al., 2003; Porro et al., 2010; Rabenstein et al., 2005; Ruediger et al., 2011).

Similar to the plasticity exhibited by the NMJ during development, the morphogenesis of epithelia involves what has been referred to as "epithelial plasticity" in which cell–cell adhesions are disassembled and cells become motile, for example in epithelial–mesenchymal transitions (Thiery and Sleeman, 2006). The acquisition of motility by epithelial cells is also involved in tumor cell invasion and metastasis. The *Drosophila* follicular epithelium is a model for studying both developmental and pathological epithelial plasticity, and recent observations indicate that Dlg and Fas2 collaborate to prevent inappropriate invasion of follicle cells between neighboring germ cells (Szafranski and Goode, 2007; Wu et al., 2008). Furthermore, border cell migration, an invasion of a subset of follicle cells between germ cells occurring during normal oogenesis, requires downregulation of Fas2 expression in the border cells (Szafranski and Goode, 2007). PAR-1 is required for detachment of border cells from the follicular epithelium and it is interesting to speculate that this might involve regulation of Dlg localization (McDonald et al., 2008). These various results indicate that regulation of the Dlg/Fas2 complex is important for the epithelial plasticity exhibited by follicle cells and this mechanism likely applies to epithelia in the developing embryo. As in muscle, Hts over-expression causes elevated levels of PAR-1 and CaMKII in epithelial cells. While Hts over-expression does not cause discernible Dlg delocalization in the epidermis, it disrupts the membrane localization of Dlg in amnioserosa cells. Dlg in the amnioserosa might be particularly susceptible to Hts function, as it is not incorporated into septate junctions in this tissue, unlike in the epidermis (Tepass and Hartenstein, 1994). Furthermore, if the delocalization of Dlg by Hts is CaMKII-dependent, it would be more pronounced in the amnioserosa than the epidermis as Hts can only weakly promote CaMKII accumulation in the epidermis. In addition to showing that Hts can regulate Dlg localization in the amnioserosa, we have determined that proper cortical localization of Hts in amnioserosa cells in the early stages of dorsal closure is dependent on Dlg. This result suggests that where Dlg and Hts are together in a complex, Dlg stabilizes the membrane localization of Hts. This stabilization may occur in cells other than the amnioserosa but might not be readily detectable. Hts localizes all around the epithelial membrane, with much of it not co-localizing with Dlg. In the very flat, squamous cells of the amnioserosa early in dorsal closure, the proportion of lateral membrane Hts dependent on Dlg for stabilization may be greater than in more columnar epithelial cells such as those in the epidermis.

Consistent with the effects that they have on each other's localization, the frequency of cuticle defects we see in *dlg hts* zygotic double mutant embryos suggests that Hts and Dlg co-operate in epithelial development, and it is of interest that mammalian adducin has recently been implicated in the stabilization and remodeling of epithelial junctions (Naydenov and Ivanov, 2010). Embryos deficient in Hts likely have a diminished ability to delocalize Dlg, effectively reducing the pool of Dlg available for de novo junction formation, and this situation would be worsened by reducing Dlg levels with a *dlg* allele. Conversely, reducing Dlg in an embryo deficient in Hts may further compromise Hts function through effects on Hts membrane localization. One of the phenotypes that we see in *hts* mutants, the frequency of which is increased by additionally reducing Dlg, is that of embryos which secrete only small pieces of cuticle. This phenotype is characteristic of maternal zygotic *dlg* mutant embryos (Bilder et al., 2000).

The interaction of Hts with Dlg suggests that adducin could be a regulator of the septate junction and it will be of interest to examine

adducin effects on septate junction morphology in the nervous system. In the *Drosophila* nervous system septate junctions are formed between glial cells, whereas in mammals they are found between glial and neuronal membranes at the paranodal junction (reviewed in (Banerjee et al., 2006)). Interestingly, β-adducin was recently identified as a paranodal junction protein localized to the neuronal membrane where it co-localizes with NCP1, the vertebrate homolog of the *Drosophila* septate junction protein Neurexin IV (Ogawa and Rasband, 2009).

Acknowledgments

We thank D. Brink for instructing us in body wall preparations, S. Bahri and T. Aigaki for fly stocks, E. Verheyen for comments on the manuscript, L. Cooley, A. Ephrussi, L. Griffith, B. Lu and the Developmental Studies Hybridoma Bank for antibodies, and A. Ribeiro for technical assistance. This work was supported by grants from the Natural Sciences and Engineering Research Council of Canada (C. K.) and the Canadian Institutes of Health Research (N. H.).

References

Arquier, N., Perrin, L., Manfruelli, P., Semeriva, M., 2001. The *Drosophila* tumor suppressor gene *lethal(2)giant larvae* is required for the emission of the Decapentaplegic signal. Development 128, 2209–2220.

Ataman, B., Budnik, V., Thomas, U., 2006. Scaffolding proteins at the *Drosophila* neuromuscular junction. Int. Rev. Neurobiol. 75, 181–216.

Bahri, S., Wang, S., Conder, R., Choy, J., Vlachos, S., Dong, K., Merino, C., Sigrist, S., Molnar, C., Yang, X., Manser, E., Harden, N., 2010. The leading edge during dorsal closure as a model for epithelial plasticity: Pak is required for recruitment of the Scribble complex and septate junction formation. Development 137, 2023–2032.

Banerjee, S., Sousa, A.D., Bhat, M.A., 2006. Organization and function of septate junctions: an evolutionary perspective. Cell Biochem. Biophys. 46, 65–77.

Bednarek, E., Caroni, P., 2011. β-Adducin is required for stable assembly of new synapses and improved memory upon environmental enrichment. Neuron 69, 1132–1146.

Bellen, H.J., Budnik, V., 2000. The neuromuscular junction. In: Sullivan, W., Ashburner, M., Hawley, R.S. (Eds.), *Drosophila* Protocols. Cold Spring Harbor Laboratory Press, Cold Spring Harbor, New York.

Bennett, V., Gilligan, D.M., 1993. The spectrin-based membrane skeleton and micron-scale organization of the plasma membrane. Annu. Rev. Cell Biol. 9, 27–66.

Bennett, V., Gardner, K., Steiner, J.P., 1988. Brain adducin: a protein kinase C substrate that may mediate site-directed assembly at the spectrin-actin junction. J. Biol. Chem. 263, 5860–5869.

Bilder, D., Li, M., Perrimon, N., 2000. Cooperative regulation of cell polarity and growth by *Drosophila* tumor suppressors. Science 289, 113–116.

Boillee, S., Vande Velde, C., Cleveland, D.W., 2006. ALS: a disease of motor neurons and their nonneuronal neighbors. Neuron 52, 39–59.

Budnik, V., Koh, Y.H., Guan, B., Hartmann, B., Hough, C., Woods, D., Gorczyca, M., 1996. Regulation of synapse structure and function by the *Drosophila* tumor suppressor gene *dlg*. Neuron 17, 627–640.

Chen, K., Featherstone, D.E., 2005. Discs-large (DLG) is clustered by presynaptic innervation and regulates postsynaptic glutamate receptor subunit composition in *Drosophila*. BMC Biol. 3, 1.

Chen, K., Merino, C., Sigrist, S.J., Featherstone, D.E., 2005. The 4.1 protein coracle mediates subunit-selective anchoring of *Drosophila* glutamate receptors to the postsynaptic actin cytoskeleton. J. Neurosci. 25, 6667–6675.

Ding, D., Parkhurst, S.M., Lipshitz, H.D., 1993. Different genetic requirements for anterior RNA localization revealed by the distribution of Adducin-like transcripts during *Drosophila* oogenesis. Proc. Natl. Acad. Sci. U.S.A. 90, 2512–2516.

Featherstone, D.E., Davis, W.S., Dubreuil, R.R., Broadie, K., 2001. *Drosophila* α- and β-spectrin mutations disrupt presynaptic neurotransmitter release. J. Neurosci. 21, 4215–4224.

Fehon, R.G., Dawson, I.A., Artavanis-Tsakonas, S., 1994. A *Drosophila* homologue of membrane-skeleton protein 4.1 is associated with septate junctions and is encoded by the *coracle* gene. Development 120, 545–557.

Gardoni, F., Mauceri, D., Fiorentini, C., Bellone, C., Missale, C., Cattabeni, F., Di Luca, M., 2003. CaMKII-dependent phosphorylation regulates SAP97/NR2A interaction. J. Biol. Chem. 278, 44745–44752.

Gardoni, F., Polli, F., Cattabeni, F., Di Luca, M., 2006. Calcium-calmodulin-dependent protein kinase II phosphorylation modulates PSD-95 binding to NMDA receptors. Eur. J. Neurosci. 24, 2694–2704.

Gorczyca, M., Augart, C., Budnik, V., 1993. Insulin-like receptor and insulin-like peptide are localized at neuromuscular junctions in *Drosophila*. J. Neurosci. 13, 3692–3704.

Gorczyca, D., Ashley, J., Speese, S., Gherbesi, N., Thomas, U., Gundelfinger, E., Gramates, L.S., Budnik, V., 2007. Postsynaptic membrane addition depends on the Discs-Large-interacting t-SNARE Gtaxin. J. Neurosci. 27, 1033–1044.

Grevengoed, E.E., Loureiro, J.J., Jesse, T.L., Peifer, M., 2001. Abelson kinase regulates epithelial morphogenesis in *Drosophila*. J. Cell Biol. 155, 1185–1197.

Gruenbaum, L.M., Gilligan, D.M., Picciotto, M.R., Marinesco, S., Carew, T.J., 2003. Identification and characterization of *Aplysia* adducin, an *Aplysia* cytoskeletal protein homologous to mammalian adducins: increased phosphorylation at a protein kinase C consensus site during long-term synaptic facilitation. J. Neurosci. 23, 2675–2685.

Guan, B., Hartmann, B., Kho, Y.H., Gorczyca, M., Budnik, V., 1996. The *Drosophila* tumor suppressor gene, *dlg*, is involved in structural plasticity at a glutamatergic synapse. Curr. Biol. 6, 695–706.

Harden, N., 2002. Signaling pathways directing the movement and fusion of epithelial sheets: lessons from dorsal closure in *Drosophila*. Differentiation 70, 181–203.

Harden, N., Lee, J., Loh, H.Y., Ong, Y.M., Tan, I., Leung, T., Manser, E., Lim, L., 1996. A *Drosophila* homolog of the Rac- and Cdc42-activated serine/threonine kinase PAK is a potential focal adhesion and focal complex protein that colocalizes with dynamic actin structures. Mol. Cell. Biol. 16, 1896–1908.

Harlow, E.L.D., 1999. Using Antibodies: a Laboratory Manual. Cold Spring Harbor Laboratory Press, Cold Spring Harbor, NY.

Hsu, S., Ju, G., Fan, L., 1988. The glucose oxidase-DAB-nickel method in peroxidase histochemistry of the nervous system. Neurosci. Lett. 85, 169–171.

Hu, J.H., Zhang, H., Wagey, R., Krieger, C., Pelech, S.L., 2003. Protein kinase and protein phosphatase expression in amyotrophic lateral sclerosis spinal cord. J. Neurochem. 85, 432–442.

Humbert, P.O., Grzeschik, N.A., Brumby, A.M., Galea, R., Elsum, I., Richardson, H.E., 2008. Control of tumourigenesis by the Scribble/Dlg/Lgl polarity module. Oncogene 27, 6888–6907.

Jacinto, A., Wood, W., Balayo, T., Turmaine, M., Martinez-Arias, A., Martin, P., 2000. Dynamic actin-based epithelial adhesion and cell matching during *Drosophila* dorsal closure. Curr. Biol. 10, 1420–1426.

Jan, L.Y., Jan, Y.N., 1982. Antibodies to horseradish peroxidase as specific neuronal markers in *Drosophila* and in grasshopper embryos. Proc. Natl. Acad. Sci. U.S.A. 79, 2700–2704.

Johansen, J., Halpern, M.E., Johansen, K.M., Keshishian, H., 1989. Stereotypic morphology of glutamatergic synapses on identified muscle cells of *Drosophila* larvae. J. Neurosci. 9, 710–725.

Kaltschmidt, J.A., Lawrence, N., Morel, V., Balayo, T., Fernandez, B.G., Pelissier, A., Jacinto, A., Martinez Arias, A., 2002. Planar polarity and actin dynamics in the epidermis of *Drosophila*. Nat. Cell Biol. 4, 937–944.

Koh, Y.H., Popova, E., Thomas, U., Griffith, L.C., Budnik, V., 1999. Regulation of DLG localization at synapses by CaMKII-dependent phosphorylation. Cell 98, 353–363.

Lahey, T., Gorczyca, M., Jia, X.X., Budnik, V., 1994. The Drosophila tumor suppressor gene *dlg* is required for normal synaptic bouton structure. Neuron 13, 823–835.

Lin, H., Yue, L., Spradling, A.C., 1994. The *Drosophila* fusome, a germline-specific organelle, contains membrane skeletal proteins and functions in cyst formation. Development 120, 947–956.

Lue, R.A., Marfatia, S.M., Branton, D., Chishti, A.H., 1994. Cloning and characterization of hdlg: the human homologue of the *Drosophila* discs large tumor suppressor binds to protein 4.1. Proc. Natl. Acad. Sci. U.S.A. 91, 9818–9822.

Lue, R.A., Brandin, E., Chan, E.P., Branton, D., 1996. Two independent domains of hDlg are sufficient for subcellular targeting: the PDZ1-2 conformational unit and an alternatively spliced domain. J. Cell Biol. 135, 1125–1137.

Mantovani, F., Banks, L., 2003. Regulation of the discs large tumor suppressor by a phosphorylation-dependent interaction with the beta-TrCP ubiquitin ligase receptor. J. Biol. Chem. 278, 42477–42486.

Massimi, P., Narayan, N., Cuenda, A., Banks, L., 2006. Phosphorylation of the discs large tumour suppressor protein controls its membrane localisation and enhances its susceptibility to HPV E6-induced degradation. Oncogene 25, 4276–4285.

Matsuoka, Y., Li, X., Bennett, V., 1998. Adducin is an in vivo substrate for protein kinase C: phosphorylation in the MARCKS-related domain inhibits activity in promoting spectrin-actin complexes and occurs in many cells, including dendritic spines of neurons. J. Cell Biol. 142, 485–497.

Matsuoka, Y., Li, X., Bennett, V., 2000. Adducin: structure, function and regulation. Cell. Mol. Life Sci. 57, 884–895.

McDonald, J.A., Khodyakova, A., Aranjuez, G., Dudley, C., Montell, D.J., 2008. PAR-1 kinase regulates epithelial detachment and directional protrusion of migrating border cells. Curr. Biol. 18, 1659–1667.

Mendoza-Topaz, C., Urra, F., Barria, R., Albornoz, V., Ugalde, D., Thomas, U., Gundelfinger, E.D., Delgado, R., Kukuljan, M., Sanxaridis, P.D., Tsunoda, S., Ceriani, M.F., Budnik, V., Sierralta, J., 2008. DLGS97/SAP97 is developmentally upregulated and is required for complex adult behaviors and synapse morphology and function. J. Neurosci. 28, 304–314.

Monastirioti, M., Gorczyca, M., Rapus, J., Eckert, M., White, K., Budnik, V., 1995. Octopamine immunoreactivity in the fruit fly *Drosophila melanogaster*. J. Comp. Neurol. 356, 275–287.

Narayan, N., Massimi, P., Banks, L., 2009. CDK phosphorylation of the discs large tumour suppressor controls its localisation and stability. J. Cell Sci. 122, 65–74.

Naydenov, N.G., Ivanov, A.I., 2010. Adducins regulate remodeling of apical junctions in human epithelial cells. Mol. Biol. Cell 21, 3506–3517.

Ogawa, Y., Rasband, M.N., 2009. Proteomic analysis of optic nerve lipid rafts reveals new paranodal proteins. J. Neurosci. Res. 87, 3502–3510.

Ohler, S., Hakeda-Suzuki, S., Suzuki, T., 2011. Hts, the *Drosophila* homologue of Adducin, physically interacts with the transmembrane receptor Golden goal to guide photoreceptor axons. Dev. Dyn. 240, 135–148.

Parkhouse, W.S., Cunningham, L., McFee, I., Miller, J.M., Whitney, D., Pelech, S.L., Krieger, C., 2008. Neuromuscular dysfunction in the mutant superoxide dismutase mouse model of amyotrophic lateral sclerosis. Amyotroph. Lateral Scler. 9, 24–34.

Parnas, D., Haghighi, A.P., Fetter, R.D., Kim, S.W., Goodman, C.S., 2001. Regulation of postsynaptic structure and protein localization by the Rho-type guanine nucleotide exchange factor dPix. Neuron 32, 415–424.

Peter, A., Schottler, P., Werner, M., Beinert, N., Dowe, G., Burkert, P., Mourkioti, F., Dentzer, L., He, Y., Deak, P., Benos, P.V., Gatt, M.K., Murphy, L., Harris, D., Barrell, B., Ferraz, C., Vidal, S., Brun, C., Demaille, J., Cadieu, E., Dreano, S., Gloux, S., Lelaure, V., Mottier, S., Galibert, F., Borkova, D., Minana, B., Kafatos, F.C., Bolshakov, S., Siden-Kiamos, I., Papagiannakis, G., Spanos, L., Louis, C., Madueno, E., de Pablos, B., Modolell, J., Bucheton, A., Callister, D., Campbell, L., Henderson, N.S., McMillan, P.J., Salles, C., Tait, E., Valenti, P., Saunders, R.D., Billaud, A., Pachter, L., Klapper, R., Janning, W., Glover, D.M., Ashburner, M., Bellen, H.J., Jackle, H., Schafer, U., 2002. Mapping and identification of essential gene functions on the X chromosome of *Drosophila*. EMBO Rep. 3, 34–38.

Petrella, L.N., Smith-Leiker, T., Cooley, L., 2007. The Ovhts polyprotein is cleaved to produce fusome and ring canal proteins required for *Drosophila* oogenesis. Development 134, 703–712.

Pielage, J., Fetter, R.D., Davis, G.W., 2006. A postsynaptic spectrin scaffold defines active zone size, spacing, and efficacy at the *Drosophila* neuromuscular junction. J. Cell Biol. 175, 491–503.

Pielage, J., Bulat, V., Zuchero, J.B., Fetter, R.D., Davis, G.W., 2011. Hts/Adducin controls synaptic elaboration and elimination. Neuron 69, 1114–1131.

Porro, F., Rosato-Siri, M., Leone, E., Costessi, L., Iaconcig, A., Tongiorgi, E., Muro, A.F., 2010. β-adducin (Add2) KO mice show synaptic plasticity, motor coordination and behavioral deficits accompanied by changes in the expression and phosphorylation levels of the α- and γ-adducin subunits. Genes Brain Behav. 9, 84–96.

Rabenstein, R.L., Addy, N.A., Caldarone, B.J., Asaka, Y., Gruenbaum, L.M., Peters, L.L., Gilligan, D.M., Fitzsimonds, R.M., Picciotto, M.R., 2005. Impaired synaptic plasticity and learning in mice lacking β-adducin, an actin-regulating protein. J. Neurosci. 25, 2138–2145.

Ranganayakulu, G., Elliott, D.A., Harvey, R.P., Olson, E.N., 1998. Divergent roles for NK-2 class homeobox genes in cardiogenesis in flies and mice. Development 125, 3037–3048.

Robinson, D.N., Cant, K., Cooley, L., 1994. Morphogenesis of *Drosophila* ovarian ring canals. Development 120, 2015–2025.

Ruediger, S., Vittori, C., Bednarek, E., Genoud, C., Strata, P., Sacchetti, B., Caroni, P., 2011. Learning-related feedforward inhibitory connectivity growth required for memory precision. Nature 473, 514–518.

Ruiz-Canada, C., Budnik, V., 2006. Synaptic cytoskeleton at the neuromuscular junction. Int. Rev. Neurobiol. 75, 217–236.

Sabio, G., Arthur, J.S., Kuma, Y., Peggie, M., Carr, J., Murray-Tait, V., Centeno, F., Goedert, M., Morrice, N.A., Cuenda, A., 2005. p38gamma regulates the localisation of SAP97 in the cytoskeleton by modulating its interaction with GKAP. EMBO J. 24, 1134–1145.

Sambrook, J., Fritsch, E.F., Maniatis, T., 1989. Molecular Cloning: a Laboratory Manual. Cold Spring Harbor Laboratory Press, Cold Spring Harbor, NY.

Schuster, C.M., Davis, G.W., Fetter, R.D., Goodman, C.S., 1996. Genetic dissection of structural and functional components of synaptic plasticity. I. Fasciclin II controls synaptic stabilization and growth. Neuron 17, 641–654.

Seidel, B., Zuschratter, W., Wex, H., Garner, C.C., Gundelfinger, E.D., 1995. Spatial and sub-cellular localization of the membrane cytoskeleton-associated protein α-adducin in the rat brain. Brain Res. 700, 13–24.

Shan, X., Hu, J.H., Cayabyab, F.S., Krieger, C., 2005. Increased phospho-adducin immunoreactivity in a murine model of amyotrophic lateral sclerosis. Neuroscience 134, 833–846.

Sigrist, S.J., Thiel, P.R., Reiff, D.F., Lachance, P.E., Lasko, P., Schuster, C.M., 2000. Postsynaptic translation affects the efficacy and morphology of neuromuscular junctions. Nature 405, 1062–1065.

Spradling, A.C., Stern, D., Beaton, A., Rhem, E.J., Laverty, T., Mozden, N., Misra, S., Rubin, G.M., 1999. The Berkeley Drosophila Genome Project gene disruption project: Single P-element insertions mutating 25% of vital *Drosophila* genes. Genetics 153, 135–177.

Steiner, P., Higley, M.J., Xu, W., Czervionke, B.L., Malenka, R.C., Sabatini, B.L., 2008. Destabilization of the postsynaptic density by PSD-95 serine 73 phosphorylation inhibits spine growth and synaptic plasticity. Neuron 60, 788–802.

Szafranski, P., Goode, S., 2007. Basolateral junctions are sufficient to suppress epithelial invasion during *Drosophila* oogenesis. Dev. Dyn. 236, 364–373.

Tejedor, F.J., Bokhari, A., Rogero, O., Gorczyca, M., Zhang, J., Kim, E., Sheng, M., Budnik, V., 1997. Essential role for *dlg* in synaptic clustering of Shaker K+ channels in vivo. J. Neurosci. 17, 152–159.

Tepass, U., Hartenstein, V., 1994. The development of cellular junctions in the *Drosophila* embryo. Dev. Biol. 161, 563–596.

Thiery, J.P., Sleeman, J.P., 2006. Complex networks orchestrate epithelial-mesenchymal transitions. Nat. Rev. Mol. Cell Biol. 7, 131–142.

Thomas, G.H., 2001. Spectrin: the ghost in the machine. Bioessays 23, 152–160.

Thomas, U., Kim, E., Kuhlendahl, S., Koh, Y.H., Gundelfinger, E.D., Sheng, M., Garner, C.C., Budnik, V., 1997a. Synaptic clustering of the cell adhesion molecule fasciclin II by discs-large and its role in the regulation of presynaptic structure. Neuron 19, 787–799.

Thomas, U., Phannavong, B., Muller, B., Garner, C.C., Gundelfinger, E.D., 1997b. Functional expression of rat synapse-associated proteins SAP97 and SAP102 in *Drosophila dlg-1* mutants: effects on tumor suppression and synaptic bouton structure. Mech. Dev. 62, 161–174.

Thomas, U., Kobler, O., Gundelfinger, E.D., 2010. The *Drosophila* larval neuromuscular junction as a model for scaffold complexes at glutamatergic synapses: benefits and limitations. J. Neurogenet. 24, 109–119.

Toba, G., Ohsako, T., Miyata, N., Ohtsuka, T., Seong, K.H., Aigaki, T., 1999. The gene search system. A method for efficient detection and rapid molecular identification of genes in *Drosophila melanogaster*. Genetics 151, 725–737.

Tomancak, P., Piano, F., Riechmann, V., Gunsalus, K.C., Kemphues, K.J., Ephrussi, A., 2000. A *Drosophila melanogaster* homologue of *Caenorhabditis elegans par-1* acts at an early step in embryonic-axis formation. Nat. Cell Biol. 2, 458–460.

Wada, A., Kato, K., Uwo, M.F., Yonemura, S., Hayashi, S., 2007. Specialized extraembryonic cells connect embryonic and extraembryonic epidermis in response to Dpp during dorsal closure in *Drosophila*. Dev. Biol. 301, 340–349.

Whittaker, K.L., Ding, D., Fisher, W.W., Lipshitz, H.D., 1999. Different 3′ untranslated regions target alternatively processed *hu-li tai shao* (*hts*) transcripts to distinct cytoplasmic locations during *Drosophila* oogenesis. J. Cell Sci. 112, 3385–3398.

Wilson, P.G., 2005. Centrosome inheritance in the male germ line of *Drosophila* requires *hu-li tai-shao* function. Cell Biol. Int. 29, 360–369.

Woods, D.F., Bryant, P.J., 1989. Molecular cloning of the *lethal(1)discs large-1* oncogene of *Drosophila*. Dev. Biol. 134, 222–235.

Woods, D.F., Bryant, P.J., 1991. The *discs-large* tumor suppressor gene of *Drosophila* encodes a guanylate kinase homolog localized at septate junctions. Cell 66, 451–464.

Wu, X., Tanwar, P.S., Raftery, L.A., 2008. Drosophila follicle cells: morphogenesis in an eggshell. Semin. Cell Dev. Biol. 19, 271–282.

Yue, L., Spradling, A.C., 1992. *hu-li tai shao*, a gene required for ring canal formation during *Drosophila* oogenesis, encodes a homolog of adducin. Genes Dev. 6, 2443–2454.

Zaccai, M., Lipshitz, H.D., 1996a. Differential distributions of two adducin-like protein isoforms in the *Drosophila* ovary and early embryo. Zygote 4, 159–166.

Zaccai, M., Lipshitz, H.D., 1996b. Role of Adducin-like (*hu-li tai shao*) mRNA and protein localization in regulating cytoskeletal structure and function during *Drosophila* Oogenesis and early embryogenesis. Dev. Genet. 19, 249–257.

Zhang, Y., Guo, H., Kwan, H., Wang, J.W., Kosek, J., Lu, B., 2007. PAR-1 kinase phosphorylates Dlg and regulates its postsynaptic targeting at the *Drosophila* neuromuscular junction. Neuron 53, 201–215.

Zinsmaier, K.E., Eberle, K.K., Buchner, E., Walter, N., Benzer, S., 1994. Paralysis and early death in cysteine string protein mutants of *Drosophila*. Science 263, 977–980.

Zito, K., Fetter, R.D., Goodman, C.S., Isacoff, E.Y., 1997. Synaptic clustering of Fascilin II and Shaker: essential targeting sequences and role of Dlg. Neuron 19, 1007–1016.